

# Gyrokinetic Vlasov code including full geometry of non-axisymmetric field and its application to Large Helical Device experiments

M. Nunami<sup>1</sup>, T.-H. Watanabe<sup>1,2</sup>, H. Sugama<sup>1,2</sup>, K. Tanaka<sup>1</sup>

<sup>1</sup>National Institute for Fusion Science, Toki 509-5292, Japan

<sup>2</sup>SOKENDAI, Toki 509-5292, Japan



## Abstract

We developed a new gyrokinetic Vlasov flux-tube code, GKV-X, which includes full geometrical effects of non-axisymmetric field configuration. The GKV-X incorporates full geometrical information of the non-axisymmetric confinement field, as well as Fourier components of the field obtained from MHD equilibrium code, VMEC. Using the code, we investigate the effects of three-dimensional geometry of the Large Helical Device (LHD) plasmas on the zonal flow (ZF) responses, the geodesic acoustic modes, and the ion temperature gradient (ITG) modes. From the linear calculation with linearized version of GKV-X, the effects on the growth rate, frequency, and mode structure of the ITG instability are clarified in the large poloidal wavenumber region where the finite gyroradius effect is also important, while the ZF responses are found to be less affected. The simulation results for the linear ITG modes are also compared with a high ion temperature discharges in the LHD experiments.

## Introduction

### Anomalous transport by plasma turbulence

The anomalous transport problem has been one of the central subjects addressed in the long history of the magnetic fusion research.

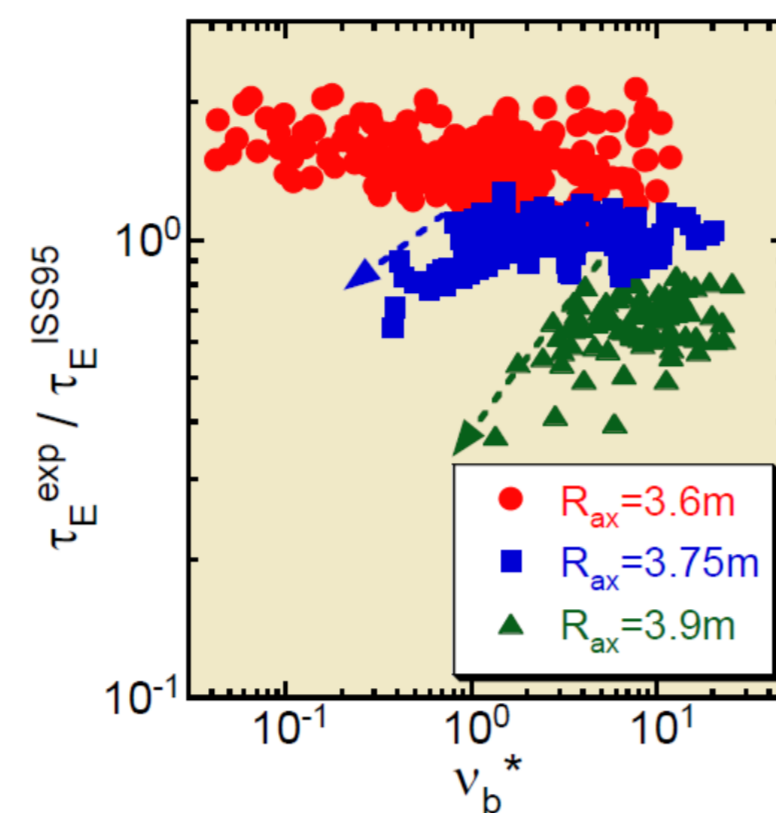
Such transport is caused by

- Turbulent transport,
- Gradients of temperatures & densities of plasmas.

### Optimized helical magnetic field

In the LHD experiment, it was observed that inward shifted LHD configuration reduced heat transport in spite of a larger amplitude of magnetic fluctuation than the outward shifted configuration.

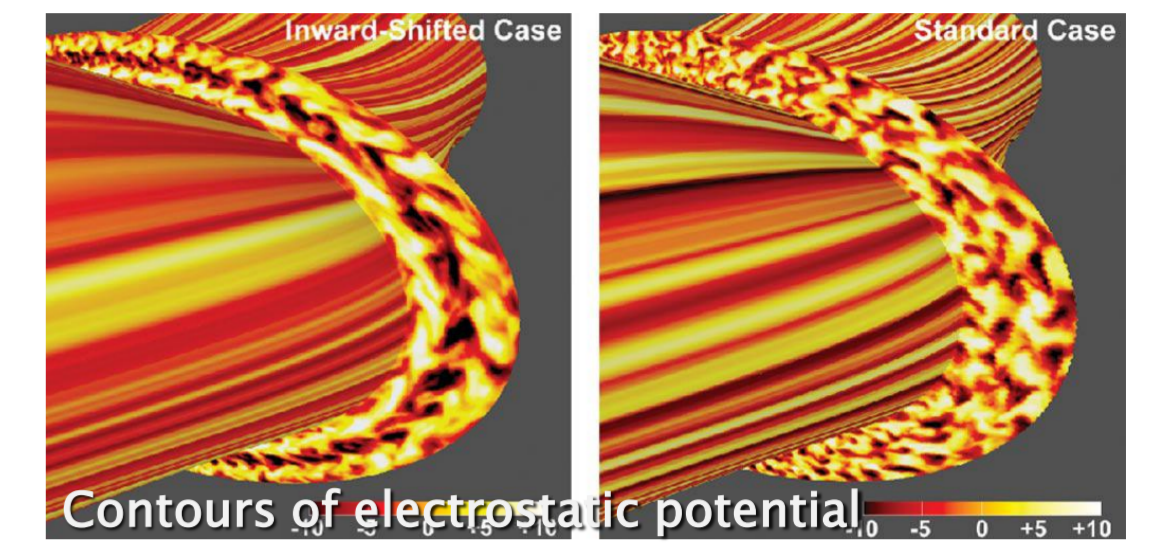
H. Yamada et al., Plasma Phys. Controlled Fusion 43, A55 (2001)



### Gyrokinetic simulation

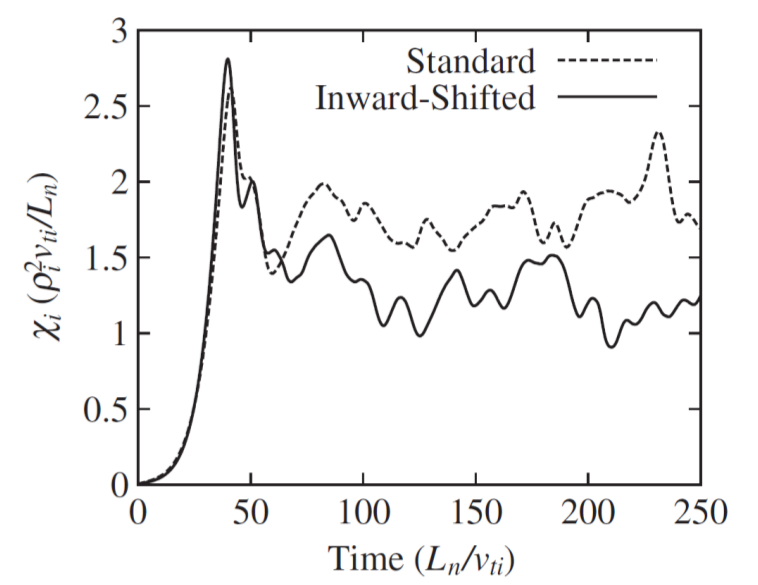
In gyrokinetic simulation with GKV code,

- In inward shifted helical model, ZFs are strongly enhanced,
- Turbulent transport is reduced by about 30% compared with standard configuration.



T.-H. Watanabe et al., Phys. Rev. Lett. 100, 195002 (2008)

For more quantitative gyrokinetic simulations, it is a natural path to furnish a well-established gyrokinetic code with detailed geometrical information obtained from three-dimensional equilibrium calculations.



## A new code "GKV-X"

M. Nunami et al., Plasma Fusion Res. 5, 016 (2010).

### "Gyrokinetic Vlasov code for quantitative comparison with experiment"

- It calculates the time-evolution of distribution function in 5D phase space due to GKE in a flux-tube domain around the field line with fixed field-line-label.
- It incorporates full geometrical information, as well as Fourier components of three-dimensional confinement field from VMEC equilibrium.

### Basic equations

#### Gyrokinetic equation

$$\frac{\partial \delta f}{\partial t} + v_{\parallel} \mathbf{b} \cdot \nabla \delta f + \frac{c}{B_0} \{ \Phi, \delta f \} + \mathbf{v}_d \cdot \nabla \delta f - \mu \mathbf{b} \cdot \nabla \Omega_i \frac{\partial \delta f}{\partial v_{\parallel}} = (\mathbf{v}_* - \mathbf{v}_d - v_{\parallel} \mathbf{b}) \cdot \frac{e \nabla \Phi}{T_i} F_M + C(\delta f)$$

(Linear & collisionless case)

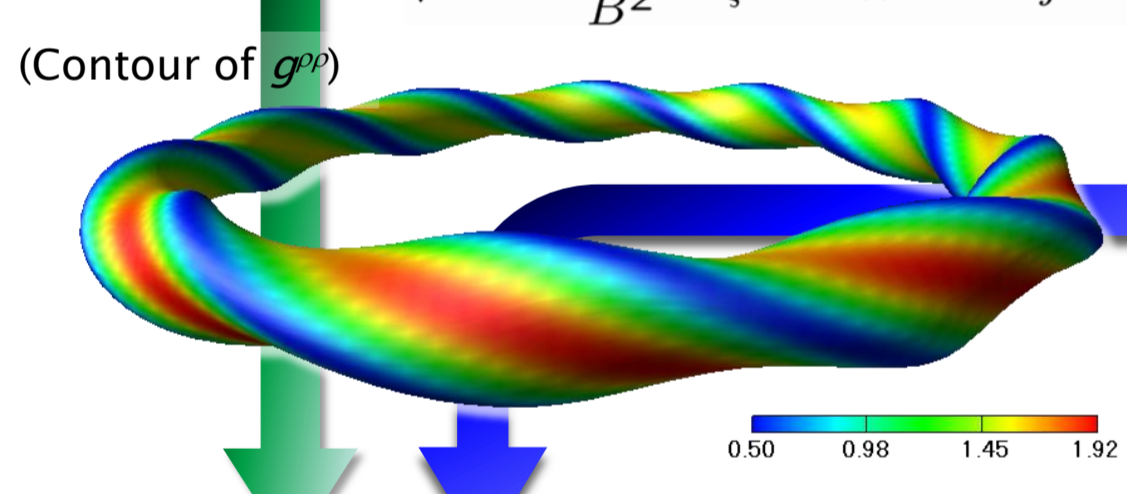
$$\left( \frac{\partial}{\partial t} + v_{\parallel} \mathbf{b} \cdot \nabla + \mu \mathbf{b} \cdot \nabla B \frac{\partial}{\partial v_{\parallel}} + i \omega_{Di} \right) f_{k_{\perp}} = f_0(-v_{\parallel} \mathbf{b} \cdot \nabla - i \omega_{Di} + i \omega_{Ti}) J_0(k_{\perp} \rho_i) \frac{e \phi_{k_{\perp}}}{T_i}$$

#### Quasi-neutrality

$$\int d^3 v J_0 \delta f_{k_{\perp}} - n_0 \frac{e \phi_{k_{\perp}}}{T_i} [1 - \Gamma_0(b)] = \begin{cases} n_0 e [\phi_{k_{\perp}} - \langle \phi_{k_{\perp}} \rangle] / T_e & \text{if } k_y = 0 \\ n_0 e \phi_{k_{\perp}} / T_e & \text{if } k_y \neq 0 \end{cases}$$

Jacobian, Metric tensor, ...

$$\sqrt{g_B} = \frac{\Psi'}{B^2} (B_{\zeta} + B_{\theta}/q), g_{ij}, g^{ij}, \dots$$



#### VMEC equilibrium (in Boozer coordinates)

$$B = \sum_{n=0}^{\infty} B_{0,n}(\rho) \cos n\zeta + \sum_{m=1}^{\infty} \sum_{n=-\infty}^{\infty} B_{m,n}(\rho) \cos(m\theta - n\zeta)$$

$$B = B_{\rho} \nabla \rho + B_{\theta} \nabla \theta + B_{\zeta} \nabla \zeta = \nabla \Psi \times \nabla \theta + q^{-1}(\rho) \nabla \zeta \times \nabla \Psi$$

Experimental data  
Temperature, density profiles, ...

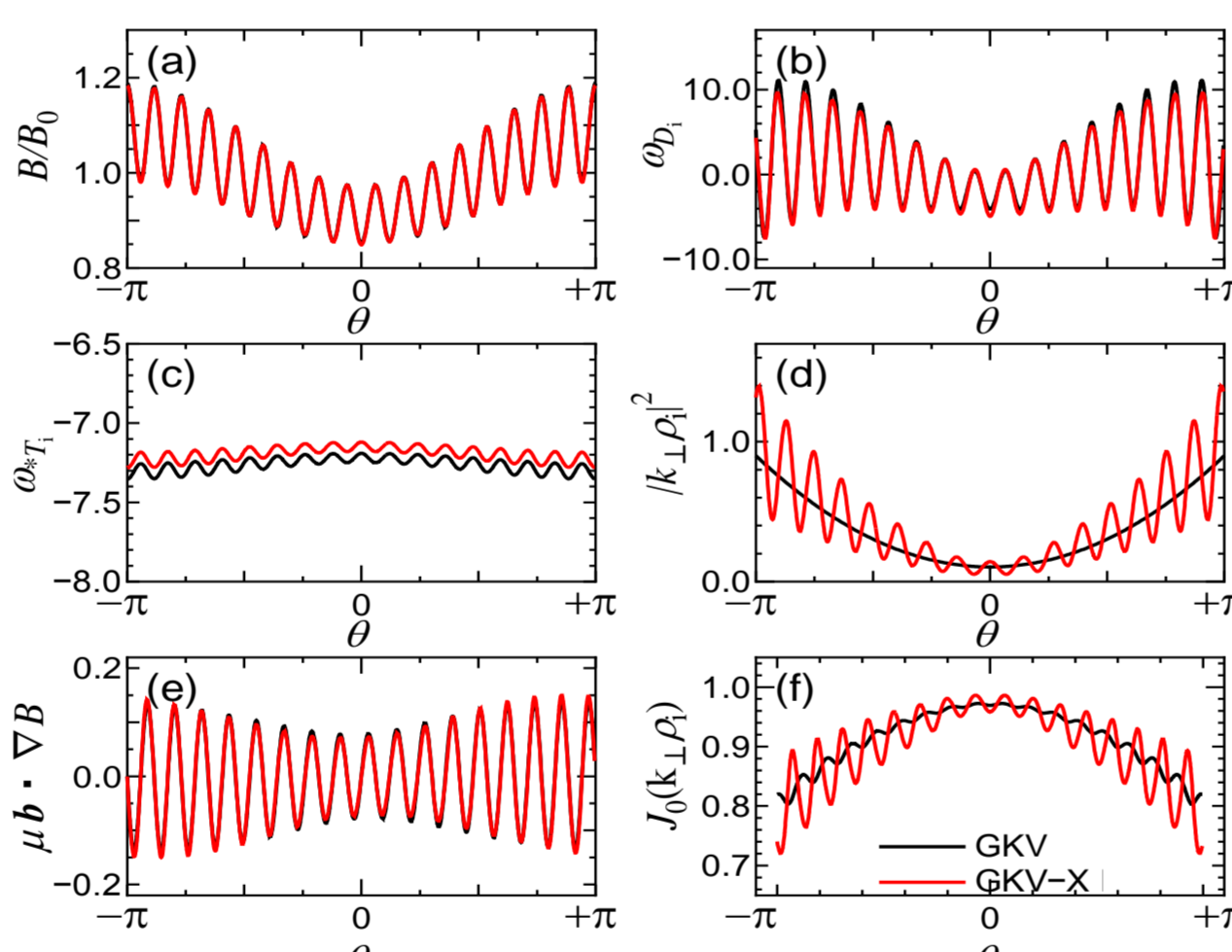
$$\omega_{Di} = -\frac{c}{eB^2} \frac{a}{\sqrt{g_B}} \left( \mu + \frac{1}{B} m v_{\parallel}^2 \right) \left[ k_y \left[ \frac{\rho_0}{q_0} B_{\rho} + \tilde{s} \theta B_{\zeta} \right] \frac{\partial B}{\partial \theta} + (\rho_0 B_{\rho} - \tilde{s} \theta B_{\theta}) \frac{\partial B}{\partial \zeta} - \frac{\rho_0}{q_0} (B_{\theta} + q_0 B_{\zeta}) \frac{\partial B}{\partial \rho} \right] + k_x \left[ B_{\zeta} \frac{\partial B}{\partial \theta} - B_{\theta} \frac{\partial B}{\partial \zeta} \right]$$

$$\omega_{*T_i} = -\frac{c T_i a^2}{e B^2 \sqrt{g_B}} (B_{\theta} + q_0 B_{\zeta}) \frac{\rho_0}{q_0} k_y \left[ \frac{1}{L_n} + \frac{1}{L_{T_i}} \left( \frac{m v^2}{2 T_i} - \frac{3}{2} \right) \right]$$

$$k_{\perp}^2 = k_x^2 a^2 g^{\rho\rho} + 2 k_x k_y a^2 \left[ \tilde{s} \theta g^{\rho\theta} + \frac{\rho_0}{q_0} (q_0 g^{\theta\theta} - g^{\rho\zeta}) \right] + k_y^2 a^2 \left[ \frac{\rho_0^2}{q_0^2} (g^{\zeta\zeta} + q_0^2 g^{\theta\theta} - 2 q_0 g^{\rho\zeta}) + 2 \tilde{s} \theta \frac{\rho_0}{q_0} (q_0 g^{\rho\theta} - g^{\rho\zeta}) + \tilde{s}^2 \theta^2 g^{\rho\rho} \right]$$

$$\mathbf{b} \cdot \nabla = \frac{\Psi'}{q_0 B \sqrt{g_B}} \left( \frac{\partial}{\partial \theta} + q_0 \frac{\partial}{\partial \zeta} \right) \quad (\tilde{s} \equiv (\rho_0/q_0)')$$

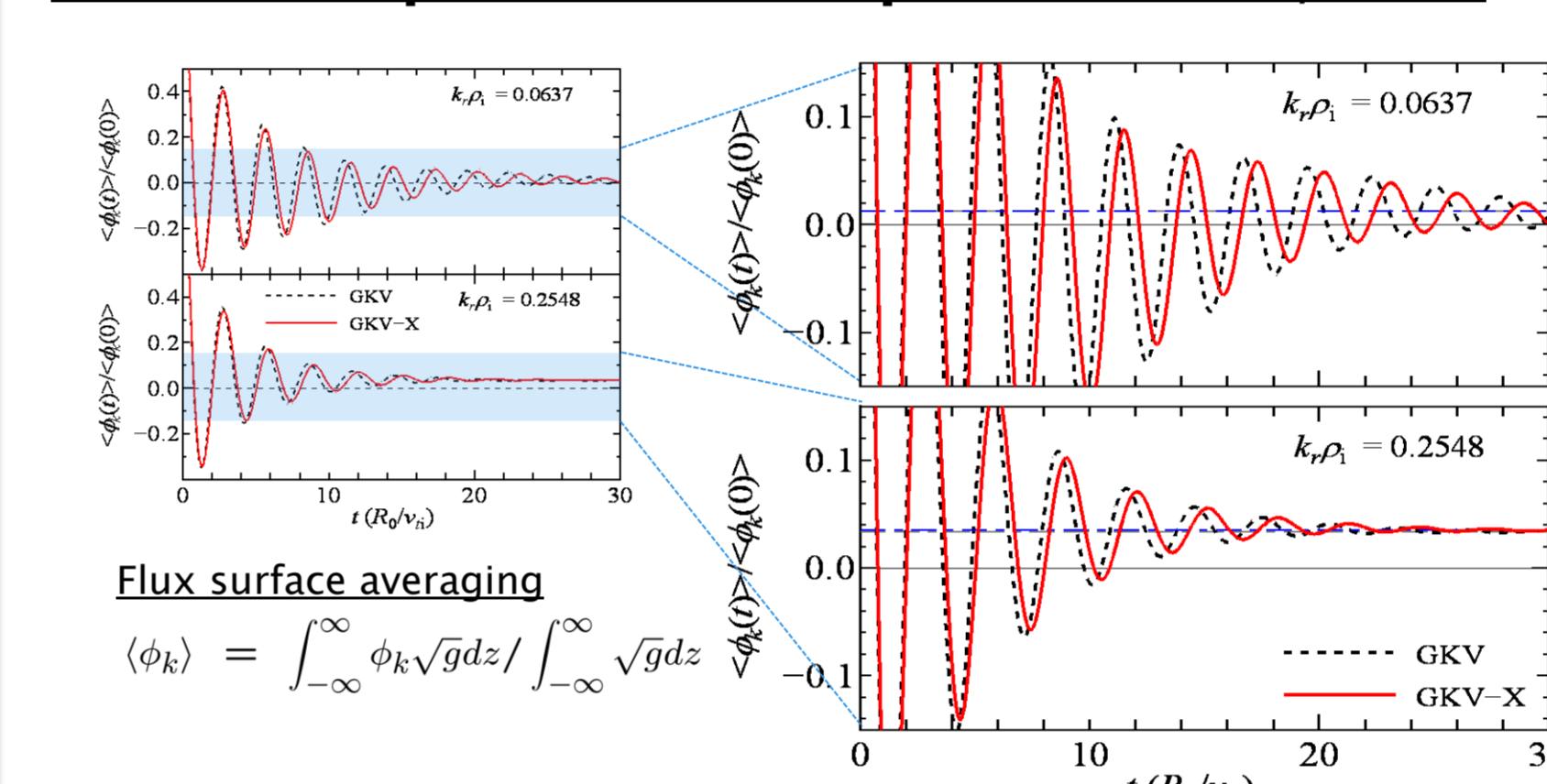
Profiles of each term for standard LHD case



## Geometrical effects on ZFs & ITG modes

To investigate the effects of non-axisymmetric geometry on the ITG modes and zonal flows, GK Vlasov simulations using linearized versions of the GKV-X and GKV codes are compared.

### Linear responses of ZF potentials ( $\rho=0.6$ )



#### Residual Levels

$$\text{For } k_r \rho_i = 0.0637 \quad \text{For } k_r \rho_i = 0.2548$$

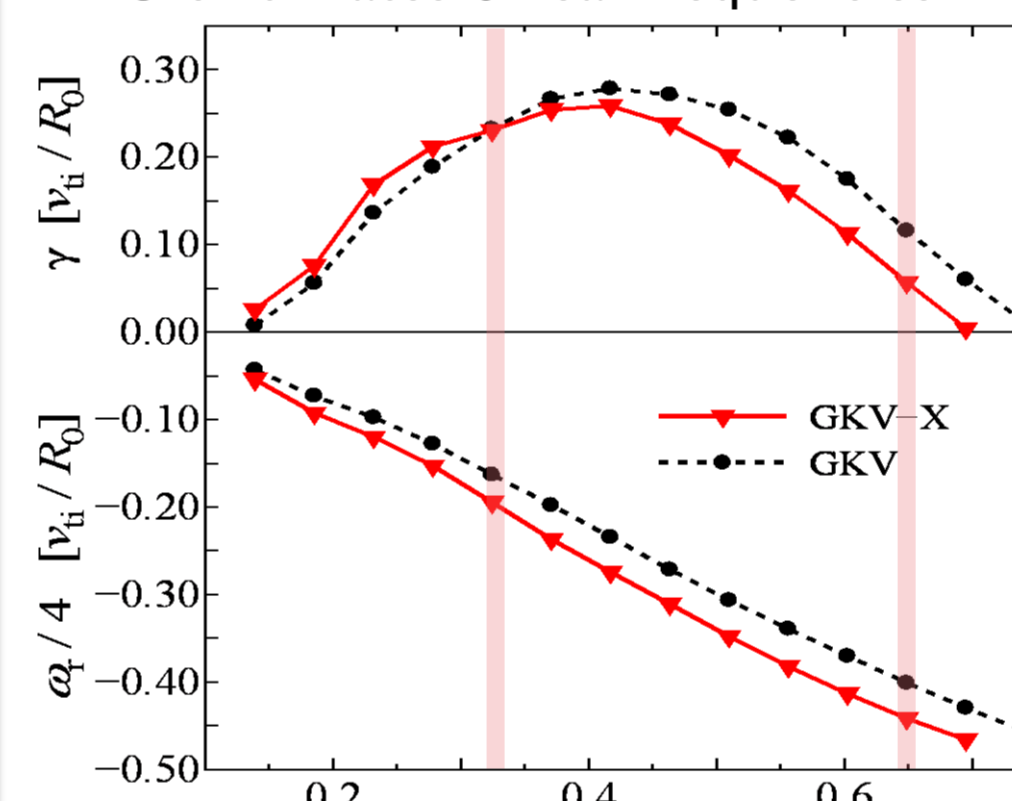
$$\mathcal{K}_{\text{GKV-X}} = 1.25 \times 10^{-2} \quad \mathcal{K}_{\text{GKV-X}} = 3.49 \times 10^{-2}$$

$$\mathcal{K}_{\text{GKV}} = 1.21 \times 10^{-2} \quad \mathcal{K}_{\text{GKV}} = 3.38 \times 10^{-2}$$

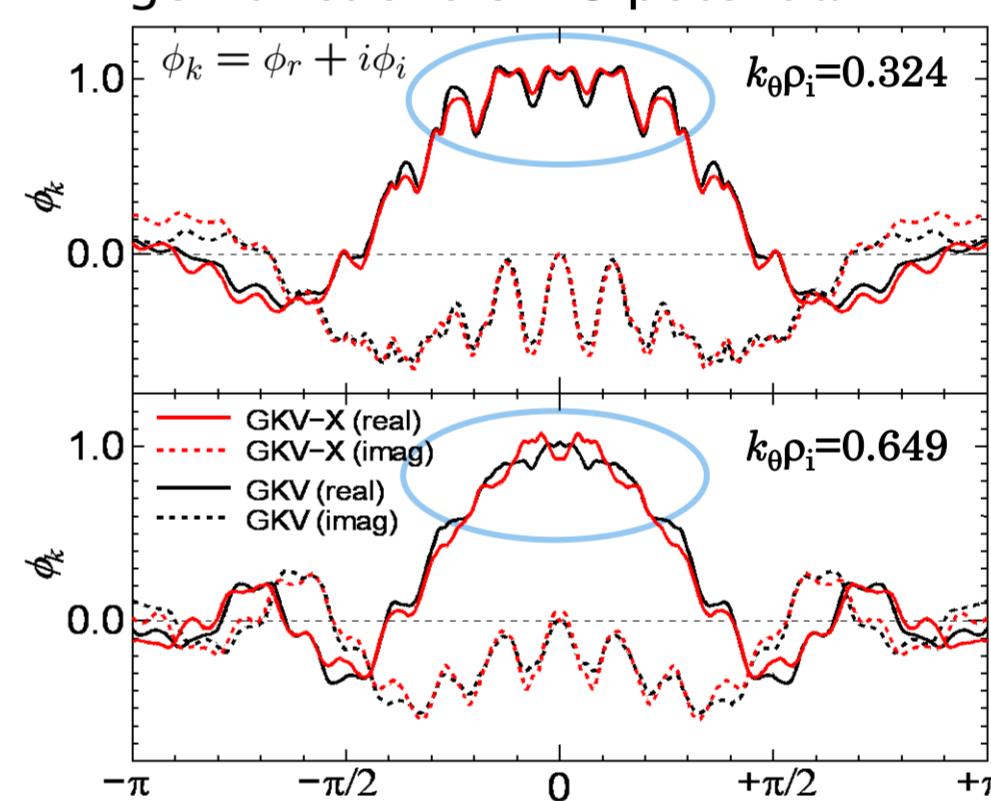
- Response functions and residual levels of ZFs agree well each other.
- We consider that the metric effect on ZFs is blinded with taking the flux surface average to determine the residual zonal flow potential.

### ITG modes ( $\rho=0.6$ )

#### Growth rates & real frequencies



#### Eigenfunctions of ES potential



- Differences between the GKV and GKV-X codes are magnified as the poloidal wave number  $k_{\theta}$  increases.
- For large poloidal wave number, the profiles have different ripple structure in the bad curvature region around  $\theta=0$ .

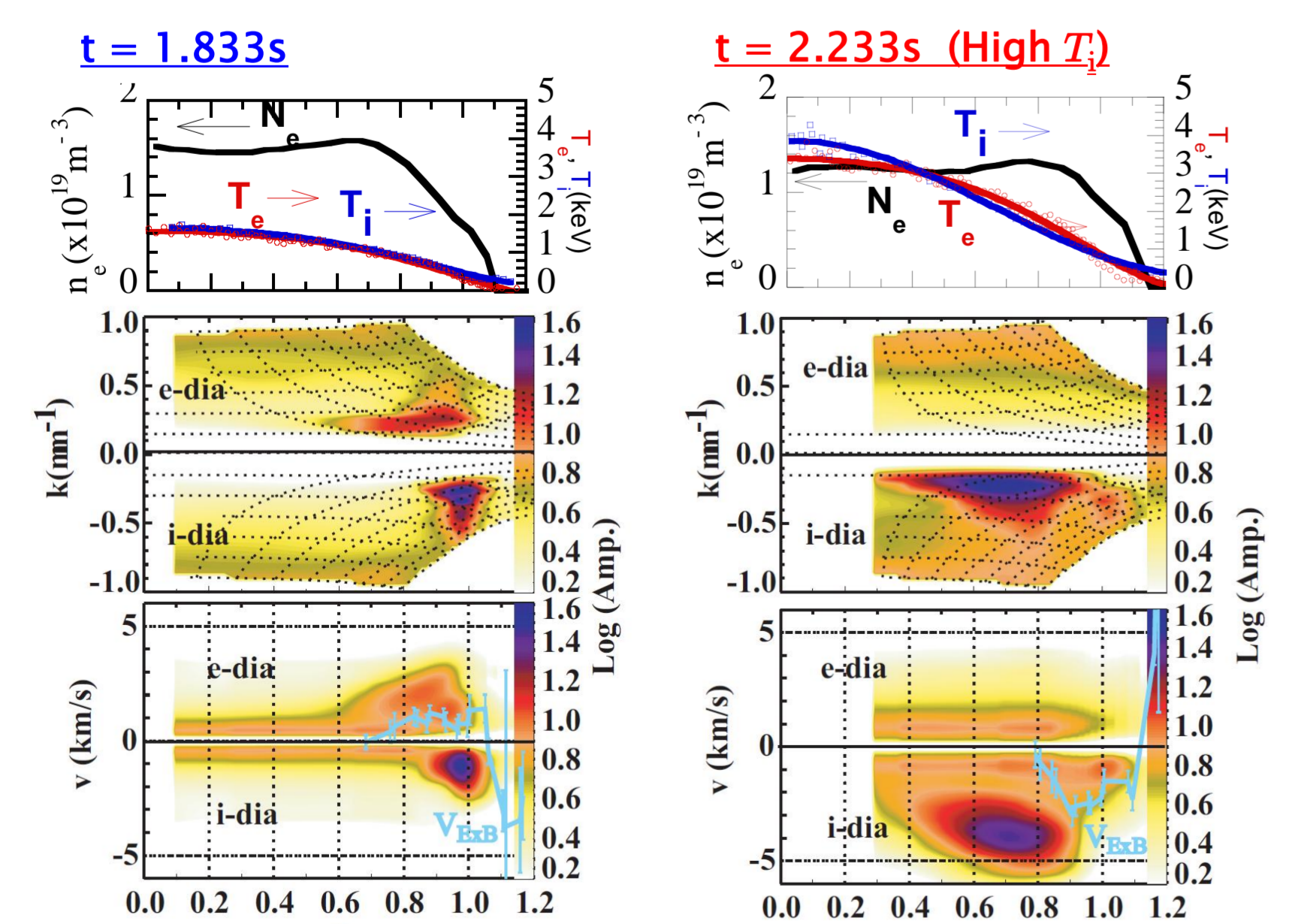
- For  $\omega_{Di}$  of the GKV-X, more helical ripple components are included, the difference appears with more negative than the GKV case.
- For  $k_{\perp} \rho_i$ , there is obvious difference.
- Differences in magnitude are enhanced for large  $k_{\theta}$ .

**Effects of full geometry & helical ripples on ITG modes are enhanced for the higher  $k_{\theta}$ .**

## Application to LHD experiment

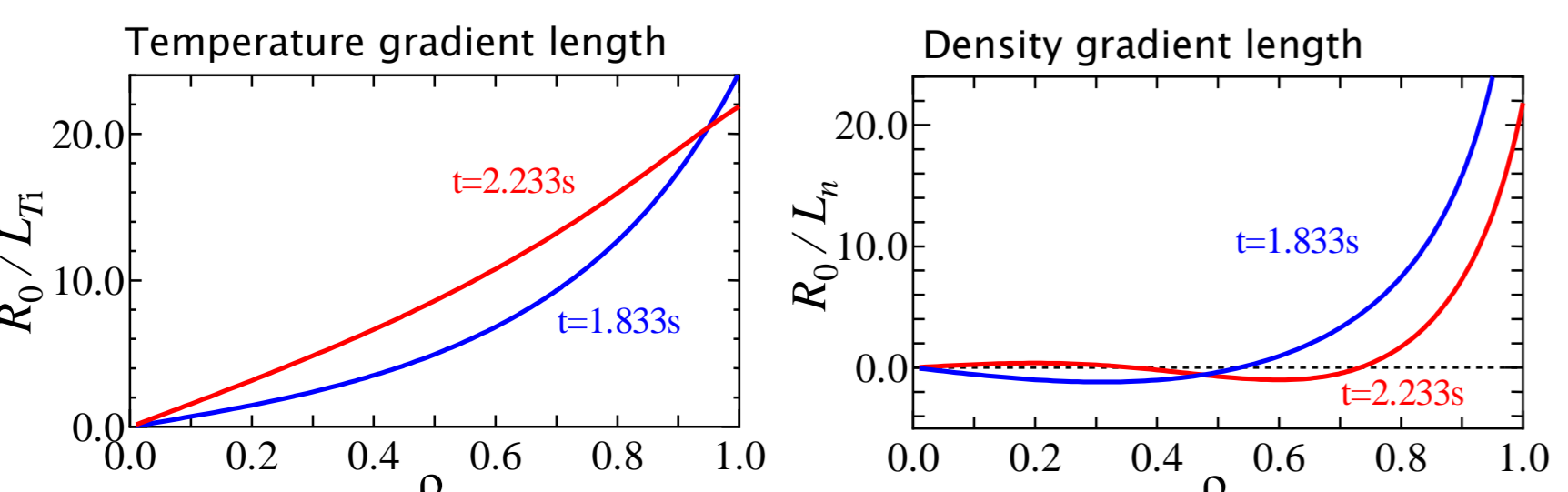
### Fluctuation in high- $T_i$ discharge in LHD

K. Tanaka et al., to be appeared in Plasma Fusion Res.



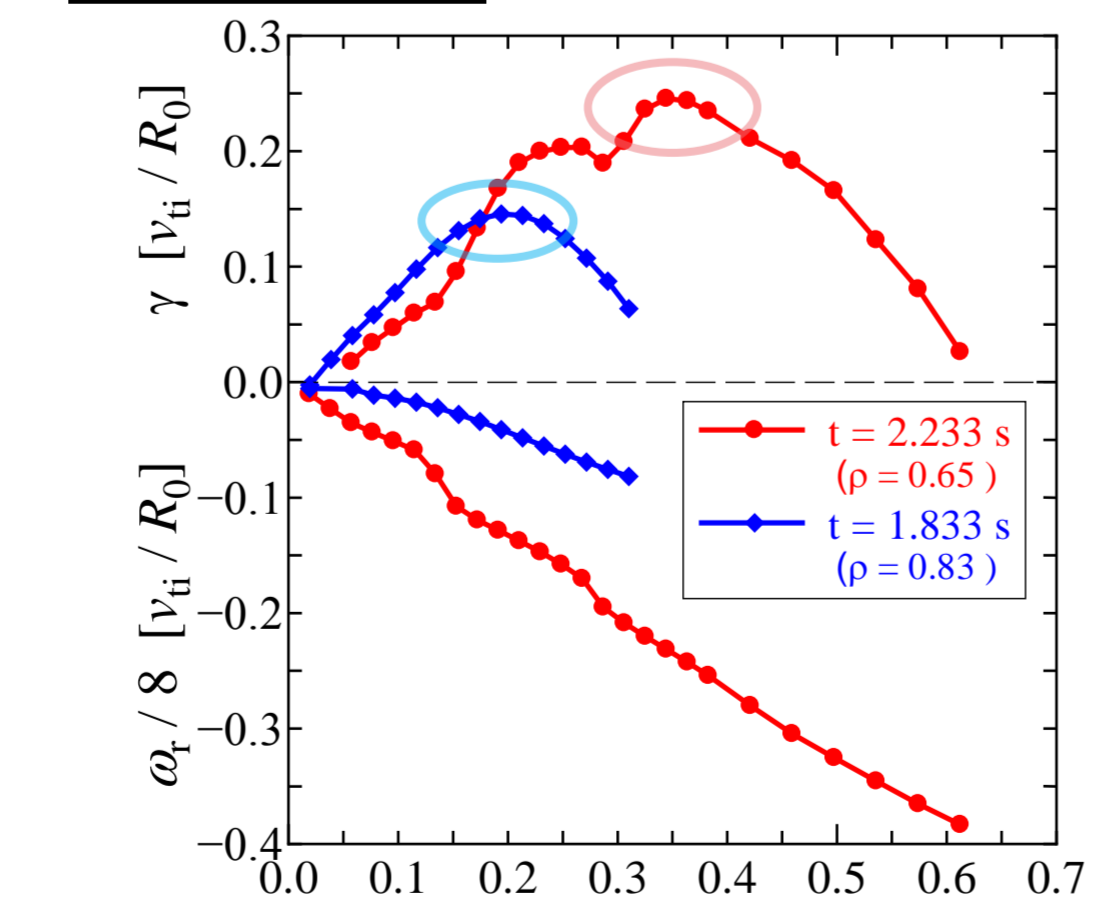
- Fluctuation peak exists at  $\rho=0.8-1.0$  in space,  $k_{\perp} \rho_i \sim 0.26$  in wavenumber.
- Fluctuation peak exists at  $\rho=0.5-0.8$  in space,  $k_{\perp} \rho_i \sim 0.45$  in wavenumber.

### Radial profiles of gradient length ( $L_X \equiv -(d \ln X / dr)^{-1}$ )



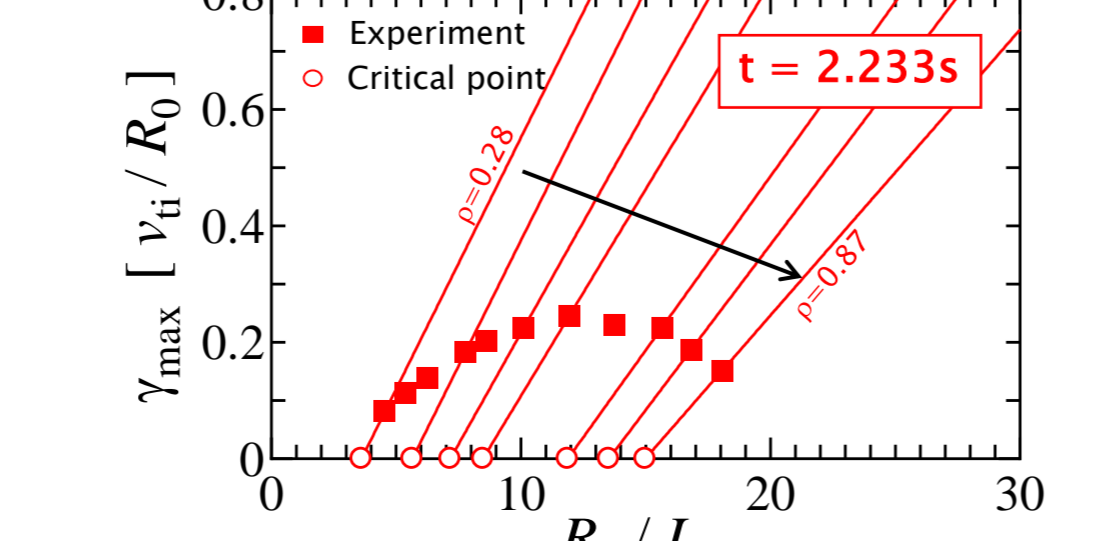
### Linear analyses by GKV-X

#### Growth rates & real frequencies of ITG modes

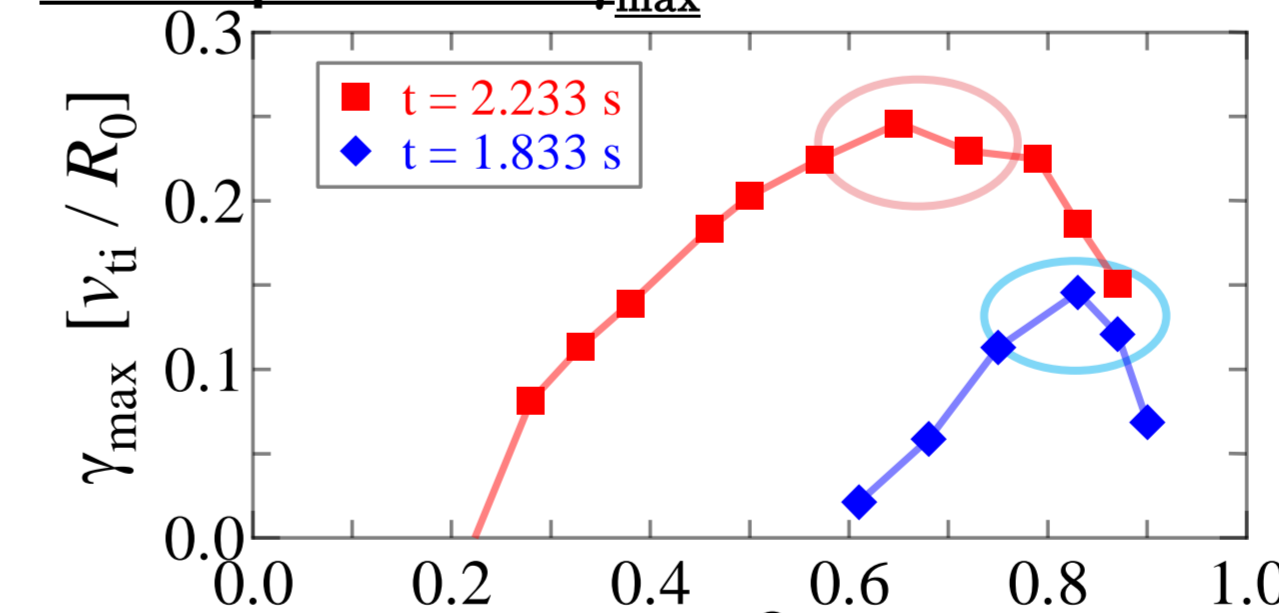


- There exists ITG unstable region.
- Maximum growth rates exist at  $k_{\theta} \rho_i \sim 0.35$  ( $t=2.233s$ ),  $k_{\theta} \rho_i \sim 0.20$  ( $t=1.833s$ ), in poloidal wavenumber space.

#### $L_{T_i}$ dependence of $\gamma_{\max}$

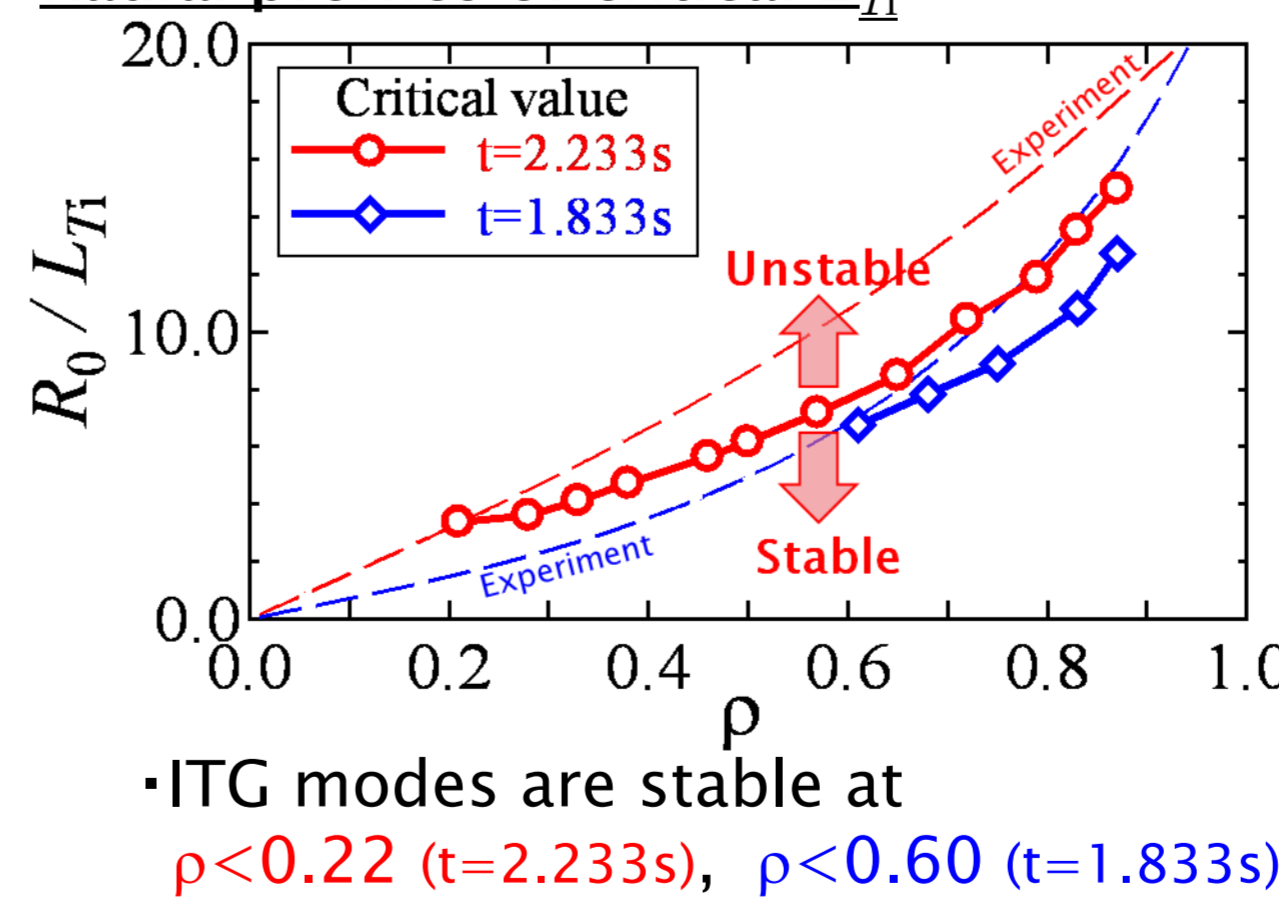


### Radial profiles of $\gamma_{\max}$



- Growth rates peak at  $\rho \sim 0.65$  ( $t=2.233s$ ),  $\rho \sim 0.85$  ( $t=1.833s$ ).

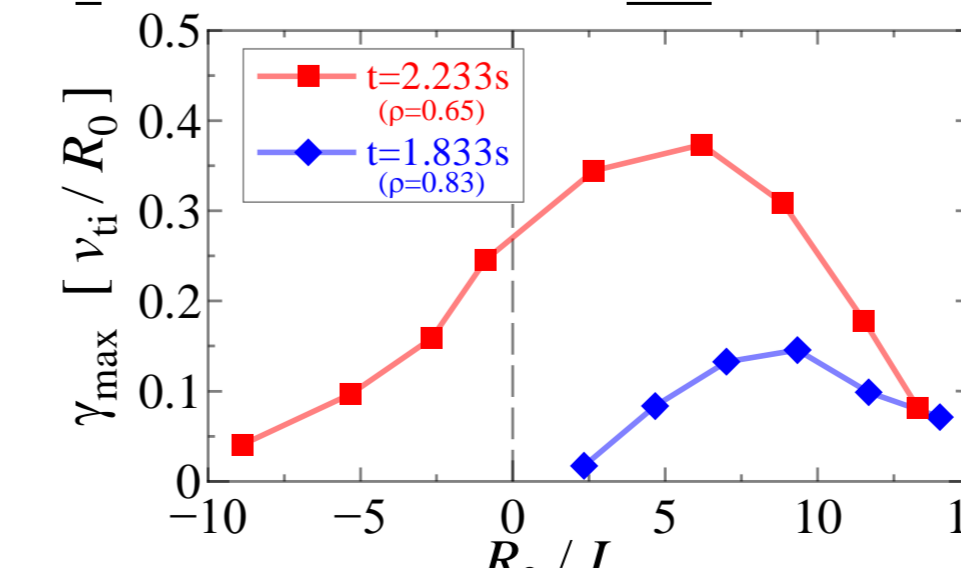
#### Radial profiles of critical $L_{T_i}$



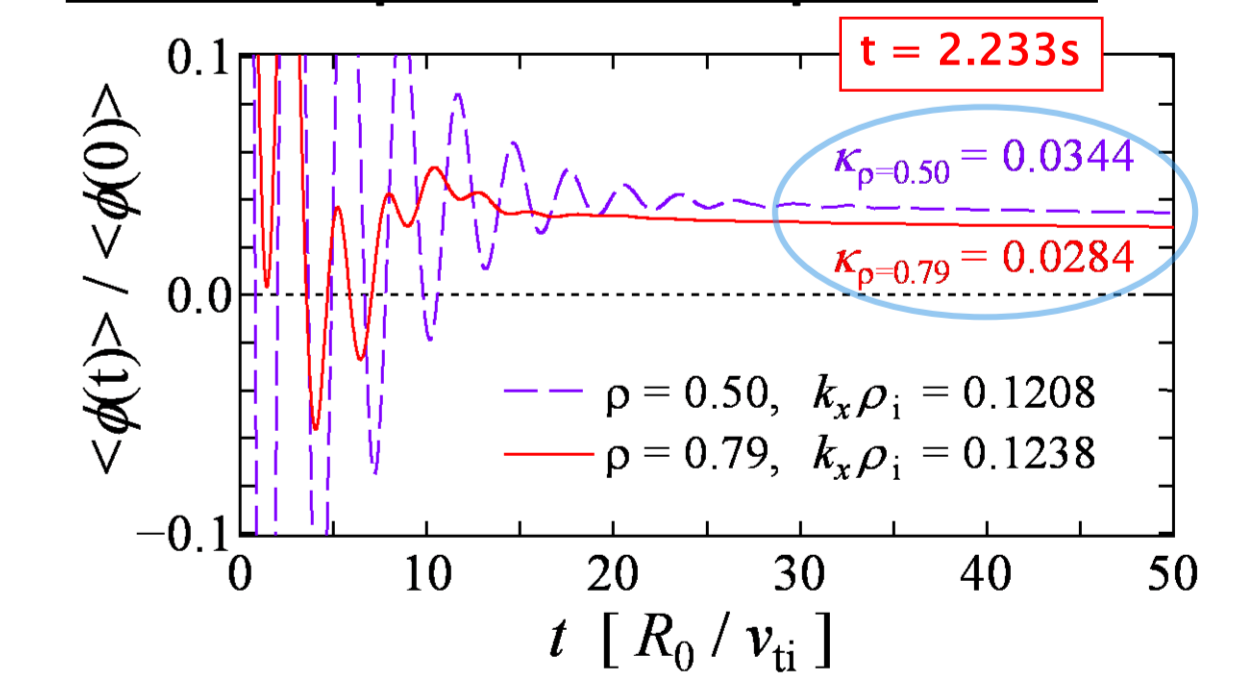
- ITG modes are stable at  $\rho < 0.22$  ( $t=2.233s$ ),  $\rho < 0.60$  ( $t=1.833s$ ).

**In High- $T_i$  phase, ITG modes are enhanced due to much steep ion temperature gradient.**

#### $L_n$ dependence of $\gamma_{\max}$



### Linear responses of ZF potentials

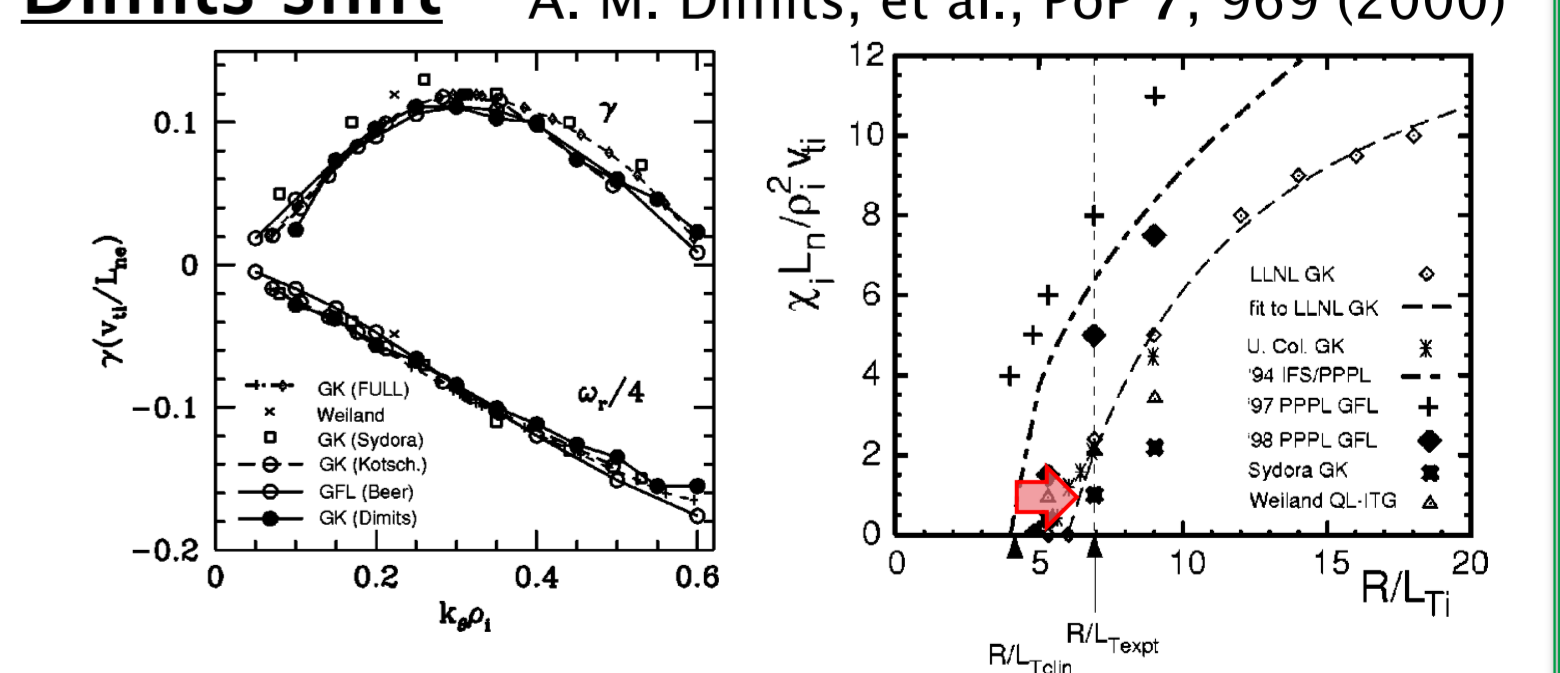


- Residual ZF level slightly increases in inner radial region.

➔ ZFs may reduce the ITG modes in inner region?

### Dimits shift

A. M. Dimits, et al., PoP 7, 969 (2000)



Now, we are analyzing turbulent transport by nonlinear GK simulation with GKV-X.

## Acknowledgement

This work is supported in part by the Japanese Ministry of Education, Culture, Sports, Science and Technology, Grant No. 22760660, and in part by the NIFS Collaborative Research Program, NIFS09KTAL022.